Temperature-induced sign reversal of biaxiality observed by conoscopy in some ferroelectric Sm-C^* liquid crystals

Jang-kun Song,[1] A. D. L. Chandani,[1] Atsuo Fukuda,[1,2] J. K. Vij,[1,*] Ichiro Kobayashi,[3] and A. V. Emelyanenko[2,4]
[1]*Department of Electronic and Electrical Engineering, Trinity College, University of Dublin, Dublin 2, Ireland*
[2]*Department of Environmental Materials Science, Tokyo Denki University, Tokyo 101-8457, Japan*
[3]*Nissan Chemical Industries, Ltd., Chiba 274-8507, Japan*
[4]*Department of Physics, Moscow State University, Moscow 119992, Russia*
(Received 22 January 2007; published 20 July 2007)

We have studied various ferroelectric liquid crystals to find the average molecular direction of the shortest axis in the perfectly unwound state by using tilted conoscopic measurements. We find that there exist two types of temperature dependencies of the biaxiality. Some materials exhibit increasing biaxiality while others show decreasing biaxiality with increasing temperature. The former shows a temperature-induced sign reversal of biaxiality. Three different physical mechanisms are identified as responsible for the emergence of biaxiality: (i) anisotropic fluctuations of the long molecular axis, (ii) a biased rotation around the long axis, and (iii) the local field effect. By means of a simple theoretical investigation, we conclude that these two types of trends are due mainly to the opposite signs of the biaxial order parameter C, which represents the second mechanism: the biased rotation around the long axis. This means that the central phenyl planes of molecules belonging to materials having biaxiality that increases with temperature are oriented on the average parallel to the tilt plane (the shortest index of refraction axis normal to the tilt plane), and, on the contrary, in those of the others molecules are oriented perpendicular to the tilt plane (the shortest index of refraction axis lying in the tilt plane). Thus, the direction of the phenyl ring plane of the liquid crystal molecules determines the different temperature dependencies of the biaxiality. It is also shown that the phenomenon of sign reversal of the biaxiality is due to the competitive contributions of the first and second physical mechanisms.

DOI: 10.1103/PhysRevE.76.011709 PACS number(s): 61.30.Gd, 42.70.Df, 77.84.Nh

I. INTRODUCTION

The biaxiality of calamitic mesogenic molecules is mainly determined by their flat hard cores. In the smectic-A (Sm-A) phase, the molecular long axes are ordered along the director, which is parallel to the smectic layer normal, while the molecular short axes specifying the core orientation are randomly distributed around the normal; hence the Sm-A phase itself is uniaxial in spite of the biaxiality of the constituent molecules. In the smectic-C (Sm-C) phase, on the other hand, the molecular long axes are ordered along the director which is tilted from the layer normal by the director tilt angle Θ. The right-handed Sm-C phase coordinate system is usually specified by fixing the Z axis parallel to the director, the Y axis perpendicular to the director tilt plane, and the X axis normal to both Y and Z. The molecular short axes must also be ordered to a certain extent due to the phase biaxiality. This quadrupolar ordering of molecular hard cores is not determined by chirality, and hence is considered to be higher than the dipolar ordering of transverse molecular dipoles in the chiral ferroelectric smectic-C (Sm-C^*) phase. Based on the assumption that the quadrupolar ordering of the molecular short axes in Sm-C is sufficiently high, Osipov and Pikin [1] developed the general phenomenological and molecular-statistical theory of Sm-C^*. They considered the influence of the quadrupolar ordering on the ferroelectric properties of Sm-C^*, and analyzed the temperature variation of spontaneous polarization, dielectric constant, and the helical pitch. Osipov and Pikin reasonably concluded: "The general situation can be clarified only after new systematic experimental investigations of the nonpolar ordering of the molecular short axes both in chiral and nonchiral smectic-C systems are carried out."

So far as the authors are aware, no direct measurement of refractive indices has proven the quadrupolar ordering of the molecular short axes in Sm-C and Sm-C^*. The smectic-C phase has been confirmed to be biaxial, as pointed out by Saupe [2] based on symmetry considerations. Let us designate the eigenaxes of the dielectric permittivities as X', Y', and Z', with the Z' axis along the largest permittivity and the $Y' \equiv Y$ axes perpendicular to the director tilt plane. Note that, in principle, the Z' and X' axes are rotated by $\delta\Theta$ about the $Y' \equiv Y$ axis with respect to the Z and X axes. Taylor *et al.* [3,4] observed $n_{Y'} > n_{X'}$(hereafter designated as positive biaxiality) in Sm-C of all the four compounds investigated by conoscopy; three of them show a first-order phase transition from isotropic to Sm-C with an almost constant tilt angle as large as 45°, and the last one apparently exhibits a second-order transition from Sm-A to Sm-C with a continuous change in the tilt angle from 0°. They concluded that at least a part of the positive biaxial character may be due to an anisotropic fluctuation of the molecular long axis, assuming molecular free rotation about this axis. Later, Galerne [5] measured all three principal refractive indices in the Sm-C as well as the Sm-A phases of another liquid crystal compound, which shows a second-order phase transition from Sm-A to Sm-C, and again confirmed that $n_{Y'} > n_{X'}$. This positive biaxiality was also interpreted on the basis of the molecular anisotropic fluctuations.

*Author to whom correspondence should be addressed. jvij@tcd.ie

More recently, many Sm-C^* compounds and mixtures have been extensively developed for FLCD ferroelectric liquid crystal display applications [6]. All of their observed melatopes in the completely unwound state emerge in the tilt plane perpendicularly to the applied field and indicate that $n_{Y'} > n_{X'}$. In this way, the previously observed biaxiality was always positive; hence no one was sure whether the short-axis-ordering contribution was really observed by clearly distinguishing it from the long-axis fluctuations. Anyway, it seems to have simply been anticipated that the short-axis ordering always occurs in such a way that the biaxiality of Sm-C and completely unwound Sm-C^* is positive ($n_{Y'} > n_{X'}$), i.e., that the melatopes in conoscopy appear parallel to the tilt plane. This anticipation is due to several facts: (i) The spontaneous polarization inevitably emerges along the C_2 axis (the Y axis) perpendicular to the tilt plane [7]; (ii) the molecular transverse dipoles must also align quadrupolarly [1]; and (iii) the most polarizable molecular short axis of the molecular core is usually considered to be parallel rather than perpendicular to the averaged direction of transverse dipoles responsible for the spontaneous polarization.

This naive belief of positive biaxiality in Sm-C^* made it easier to identify the *ferrielectric* Sm-$C_A^*(1/3)$ subphase, which shows negative biaxiality due to the special molecular ordering, in the early stages of the investigations of the subphases (the Sm-C^* variants) [8–11]. At the same time, it appeared to promote an incorrect phase identification of compounds and mixtures developed for the smectic liquid crystal display with gray scale (the so-called V-shaped switching materials) [12–14]. These materials were assigned to be *ferrielectric* by simply observing the electric field dependence of their conoscopic figures, i.e., by confirming negative biaxiality in the completely unwound state. The ferrielectric temperature range is as wide as 100 °C or more in some of these compounds and mixtures. This fact indicates that the assignment is unacceptable, because the only ferrielectric phase, whose existence is well established, is the Sm-$C_A^*(1/3)$ subphase produced by the frustration between ferro- and antiferroelectricity, and it can emerge in a temperature range as narrow as 10 °C or less. Moreover, there is no reason that Sm-C^* could not show melatopes parallel to an applied electric field in its completely unwound state. In other words, the structural symmetry of Sm-C^* allows either of the two cases: where the melatopes appear parallel or perpendicular to the field, whereas parallel melatopes inevitably appear in the ferrielectric Sm-$C_A^*(1/3)$ subphase.

This paper has a triple experimental purpose, as described in Sec. III. The first is to show that no discrepancy exists in assigning the above V-shaped switching materials as ferroelectric instead of as ferrielectric, by observing the temperature variations of Bragg reflection bands due to the helical structure [15–17]. The second is to study the temperature dependence of biaxiality rather systematically, using various compounds and mixtures, including V-shaped switching materials. We will note that all of them show positive biaxiality at high temperatures just after the phase transition to Sm-C^*, which is probably due to the fluctuations of the molecular long axis, and that some materials do exhibit a temperature-induced sign reversal of biaxiality. Finally, the third purpose is to give an exciting result which shows that the observed biaxiality scarcely depends on the enantiomeric excess (optical purity) of the sample compounds. On the basis of these three experimentally observed facts, as discussed in Sec. IV, we model actual molecules as biaxial ones with the point symmetry D_2 or D_{2h}, and analyze the local field effect. We can conclude that the negative biaxiality unambiguously results from the quadrupolar ordering of the molecular core parts. Finally, the biasing direction of molecular rotation around the long axis is considered in terms of a more realistic model based on molecules with C_1 point symmetry by taking into account two kinds of the molecule, head up and head down.

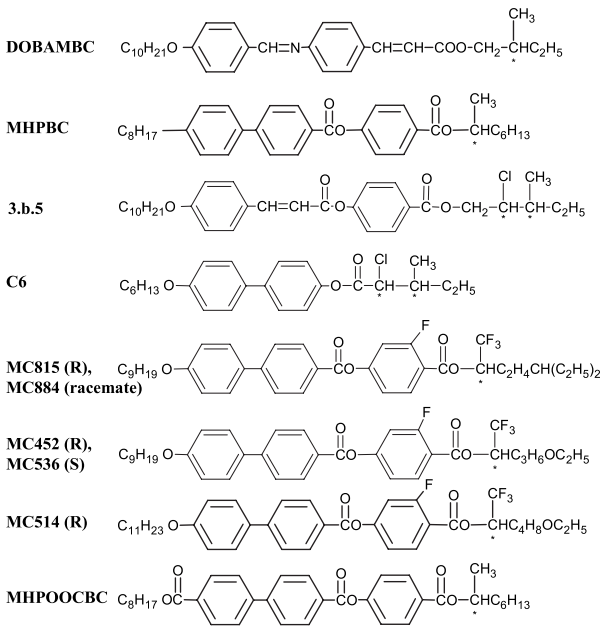

FIG. 1. Chemical structures of samples used: MC815 (R moiety), MC-884 (racemate of MC815), MC452 (R moiety), MC536 (S moiety of MC452), MC514 (R moiety). We also measured the temperature dependence of biaxiality in three mixtures, i.e., Tokyo mixture, Y102, and Felix18.

II. EXPERIMENT

The samples used are listed in Fig. 1. The V-shaped switching was first observed in the Inui mixture (sometimes also called the Tokyo mixture) [18,19], which was initially considered to be antiferroelectric, but later was regarded to be ferroelectric although some questions have been raised regarding the assignment. Mitsubishi Gas Chemical Company (MGC) developed MC815 and MC452 compounds and the Y102 mixture for V-shaped switching materials and considered them to be ferrielectric [12–14]. Note, however, that these are ferroelectric, as explained in detail in the following. Homeotropically aligned, 50–150 μm thick cells of the samples listed in Fig. 1, were prepared by using two glass plates coated with a Dow-Corning silane coupling agent [72% 3-(trimethoxysilyl)propyldimethyloctadecyl ammonium chloride and 28% methanol], for spectroscopy and

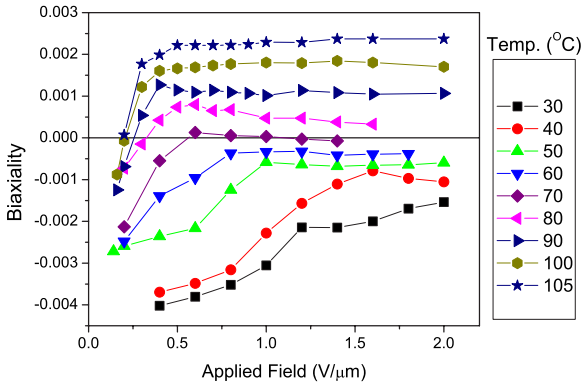

FIG. 2. (Color online) Plots of the apparent biaxiality vs applied field measured by conoscopy for MC452 at various temperatures.

conoscopy measurements. Free-standing films, ranging from 30 to 50 μm thick, were drawn across a 2 mmϕ hole drilled on a 300 μm thick steel plate for spectroscopically observing Bragg reflection bands due to the helical structure. These films were used conveniently to see the existence of reflection bands, but the observed band shape is usually disturbed by inhomogeneity in film thickness. Consequently, Bragg reflection bands were observed with a spectrometer (Perkin Elmer, Lambda 900) by using carefully prepared homeotropically aligned cells of 50–100 μm thickness.

Biaxiality was studied by conoscopy [20] using an optical polarizing microscope (Olympus BX-52). We used lenses with large numerical aperture (NA) both for the objective (Olympus, LM PlanFI; 50×0.5 NA) and the condenser (Instech; 0.65 NA). The sample was heated in an oven, which has a wide aperture to allow for large-angle conoscopic measurements to be carried out, and the sample is carefully insulated thermally with glass windows. To unwind the helical structure completely, we applied an electric field using PET spacers covered with gold foils, and these are separated by 300 μm. A wave generator and an amplifier allowed us to apply a maximum voltage of 600 V dc or ac to the sample cell, which equates to the maximum electric field of 2000 V/mm. The conoscopic image quality deteriorated seriously when some *LC* flow occurred. To minimize the flow effect, we were very careful in sample handling and utilized a 1 Hz square wave field instead of a dc signal. The conoscopic images obtained were analyzed to get the biaxiality $(n_{Y'}-n_{X'})$. The method of analysis was basically similar to that used by Gorecka *et al.* [8] and its details were explained in the previous paper [20]. We plotted apparent biaxiality vs applied field for MC452 as illustrated in Fig. 2 and confirmed the complete unwinding of the helical structure. As seen in Fig 2, the biaxiality at low applied fields is quite low, and increases rather rapidly with electric field, and then saturates to a constant value at high fields. This is commonly observed during the unwinding process of the Sm-C^* phase [20,36]. The observation of the positive biaxiality as the saturated value for the unwound Sm-C^* is quite normal, whereas the negative biaxiality is an unusual but interesting observation.

The numerical aperture of 0.5 corresponds to an angular field of −30° to +30° in air, i.e., −19.5° to +19.5° in a liquid

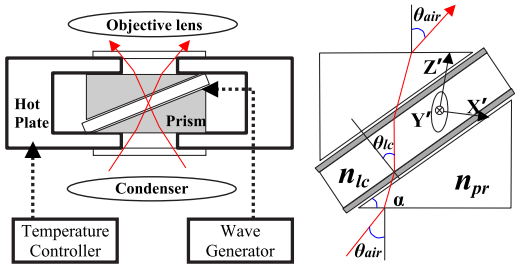

FIG. 3. (Color online) Modified experimental setup of conoscopy using a tilted cell and high refractive index prisms made up of heavy optical glass; assembly inserted into a special hot stage.

crystal with $n_{LC}=1.5$, contained in a sample cell placed horizontally on the microscope stage. Consequently, the melatopes of MHPOOCBC having the tilt angle of approximately 25° are out of the field of view, so that we could not determine the biaxiality. By sandwiching the cell between a pair of prisms made of heavy optical glass (SF11), as illustrated in Fig. 3, with an index of refraction of 1.82 and an apex angle of 30°, we attained an angular field ranging from 17° to 60.6°, and improved this weak point of the limited tilt angle for which so far the biaxiality measurement could only be made; here index-of-refraction matching oil was used to reduce the reflection resulting from the air gaps between the glass plates and the prisms. For some experiments, the two prisms were replaced with metal attachments, which hold a conventional cell slanted by 30° with respect to the microscope stage, so that the angular field in the sample liquid crystal varies from 0° to 35.3°. In this way, we can use conoscopy for measuring biaxiality as large as ±0.004 in Sm-C^*, when the tilt angle is also as large as 45°.

Snell's law assures that a ray traveling in air at an angle of θ_{air} with respect to the microscope optical axis makes an angle θ_{LC} from the smectic layer normal, given by

$$\theta_{LC} = \sin^{-1}\left\{\sin\left[\sin^{-1}\left(\frac{\sin\theta_{air}}{n_{pr}}\right)+\alpha\right]\frac{n_{pr}}{n_{LC}}\right\}. \quad (1)$$

Here n_{pr} and α are the index of refraction of the prism and its apex angle, and n_{LC} is the index of refraction of the sample liquid crystal. This equation obtained for the prism-sandwiched cell is also applicable to that of a slanted cell as well as to a conventional cell placed horizontally on the microscope stage, where α is 30° and zero, respectively, and $n_{pr}=1$ for both cases.

III. RESULTS

A. The correct assignment of ferroelectric Sm-C^* for V-shaped switching materials

Y102 is a mixture developed by MGC for V-shaped switching, which was used by Casio as a prototype of a 5.5 in., full-color, video rate LCD [12]. Although the ingredients of Y102 are proprietary to the company, an MGC patent applications [14] appears to indicate that the two main components are MC815 and an antiferroelectric compound (MC881), and that the mixing ratio is close to the critical

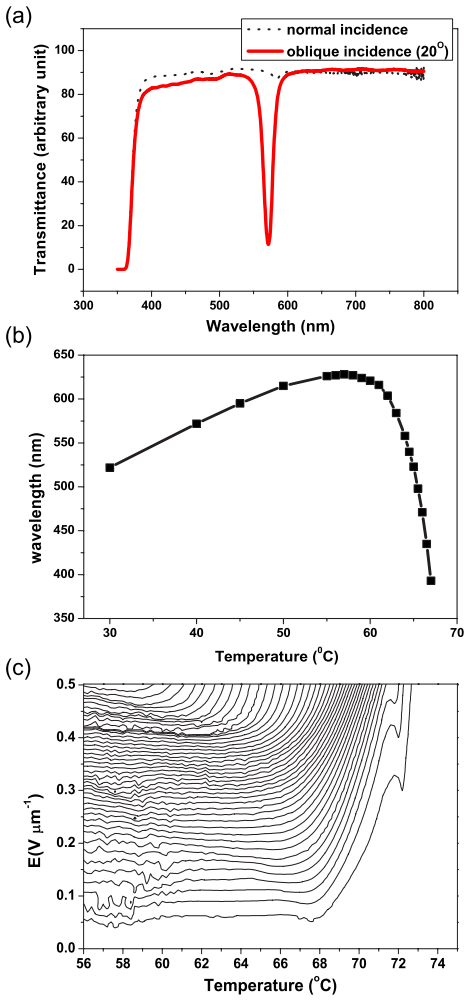

FIG. 4. (Color online) Experimental data of Y102 obtained by using homeotropic cells. (a) Reflection band at 40 °C (100 μm homeotropic cell) for normal and oblique incidence of light. (b) Temperature dependence of the peak of the full-pitch reflection band (100 μm homeotropic cell). (c) Field-induced birefringence contour lines in *E-T* space obtained by using a PEM. Lines shown are those of constant birefringence $10^{-3}\Delta n$. This shows a Sm-C^* phase up to a temperature of 68 °C, followed by Sm-C^*_α from 68 to 72 °C and a Sm-*A* phase at higher temperatures.

concentration where the ferrielectric and the antiferroelectric phases have equal free energies. Note that this critical concentration scarcely depends on the temperature, as illustrated in Fig. 1 of Ref. [14]. Since MGC considered Y102 to be ferrielectric and, moreover, since this assignment must be inappropriate as pointed out in Sec. I, we first studied the Bragg reflection of Y102 in detail as a function of temperature. Only one peak is observed in the wavelength region of 350 nm–2.5 μm over a wide temperature range from below 0 °C upto 68 °C and the band shape is ideally bell shaped as illustrated in Fig. 4(a). The band peak changes smoothly with temperature as shown in Fig. 4(b). No jump in the wavelength of the Bragg reflection occurs, which suggests that no phase transition is observed, except for the very steep decrease of helical pitch at high temperatures just below the Sm-*A* phase. The steep decrease in the wavelength of the selective reflection (a measure of the helical pitch) suggests the existence of Sm-C^*_α in a narrow temperature region just below Sm-*A* [21]. In fact, the birefringence contour lines drawn in the *E-T* space using a photoelastic modulator (PEM) clearly proves the existence of Sm-C^*_α as shown in Fig. 4(c). Aside from this narrow temperature range, it is natural to consider that Y102 shows a single phase in a wide temperature range, and that this phase should be assigned as ferroelectric Sm-C^*.

Now let us examine whether the Bragg reflection due to the helical structure can reasonably be understood by identifying this phase as ferroelectric Sm-C^*. The dispersion relation for Sm-C^*, as studied in detail by Ouchi *et al.* [17], naturally depends on the director's tilt angle and the light propagation direction specified by an oblique angle from the helical axis, i.e., the smectic layer normal. The first-order reflection, which is called the full pitch band, shows total reflection. It emerges at a wavelength equal to about twice the optical helical pitch (mechanical pitch times average index of refraction, $\bar{n}p$) when the light is incident almost normally to the smectic layer and propagates nearly parallel to the helical axis. Note that the reflection intensity becomes zero, and the full-pitch band is not observed for exact normal incidence. The second-order reflection, called the characteristic band, corresponds to the first-order reflection in the chiral nematic (cholesteric) phase, and it has a much more complicated dependence on the tilt angle and on the oblique propagation (incidence angle) direction. It is generally a triplet, with a central total reflection band, and characteristic selective reflection bands appearing on both sides of it. For normal incidence, these three bands coalesce, the central band becomes infinitesimally narrow, and the second-order reflection is circularly polarized.

The single reflection band observed in Y102 must be the full-pitch band in Sm-C^* because its intensity is much stronger than 50%, and the reflected light is not circularly polarized. Some investigators have been skeptical about this identification, however, noticing in particular that the single reflection in Y102 did not completely disappear even for normal incidence of the light. This may be an artifact, which is caused by the nonideal situation of an ordinary experimental setup to measure the reflection band using a spectrometer or a spectrophotometer. The light beam passing through a sample liquid crystal is not an ideal plane wave but a convergent one; some rays may propagate through the sample obliquely at angles of a few degrees with respect to the helical axis. The second-order characteristic reflection band must be hidden in the opaque intrinsic absorption region of the liquid crystal mixture Y102. In the case of MC815, the appropriateness of identifying the phase as ferroelectric Sm-C^* is much clearer. Figure 5 shows the wavelength of the reflection peaks vs. temperature. Two reflection bands are observed at higher temperatures; with decreasing temperature, the second reflection band gets buried in the opaque intrinsic absorption region. The first reflection band peak varies smoothly with temperature; no jump in the wavelength of the reflected light occurs, which suggests that no phase transition is observed over a wide temperature range from below room temperature up to 100 °C where the phase transition to isotropic occurs. Therefore, it is quite reasonable to conclude

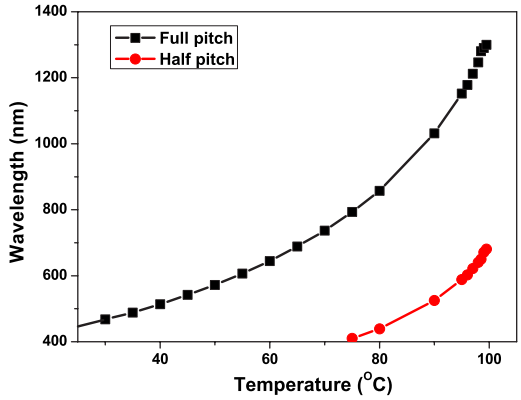

FIG. 5. (Color online) Observed temperature dependencies of the peaks of the two reflection bands of MC815.

that MC815 exhibits Sm-C^* over a wide temperature range. Contrary to the case for Y102, there exists neither Sm-C^*_α nor Sm-A in MC815 just below the isotropic phase. For normal incidence, the first-order reflection is practically zero, but the second-order one shows a saturation at 50% and is polarized circularly with right handedness for the R moiety.

B. Temperature dependencies of biaxiality

Figure 6 summarizes the results for the temperature dependence of the observed biaxiality in the unwound Sm-C^* of the various compounds and mixtures listed in Fig. 1. Two types of temperature dependency are observed; the biaxiality decreases with increasing temperature in Fig. 6(a), while it increases with temperature in Fig. 6(b), except, sometimes, for a narrow high-temperature region of Sm-C^*. For example, MHPBC, Felix18, C6, etc. (let us designate these materials as group A for convenience) have biaxiality that decreases with increasing temperature, and MHPOOCBC, Y102, MC815 etc. (designated as group B) show an increasing trend except in a narrow temperature region. Group B has negative biaxiality values at low temperatures, with a change in the sign of the biaxiality above a certain temperature. So these compounds become uniaxial at a certain intermediate temperature depending on the wavelength of the light used for conoscopy. That is also seen in Fig. 7, which shows conoscopic images, where the melatopes in conoscopy change

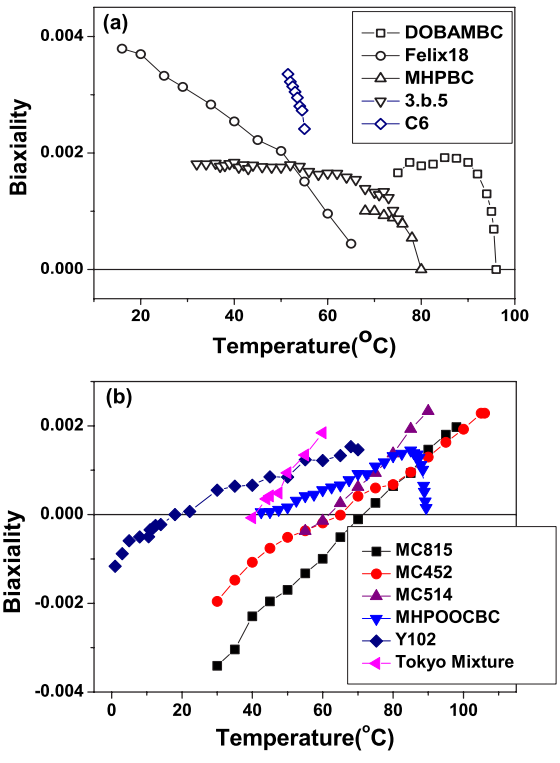

FIG. 6. (Color online) Two types of temperature dependencies of biaxiality: (a) decreasing biaxiality with increasing temperature for compounds given in the inset; (b) increasing biaxiality with increasing temperature and temperature-induced sign reversal of biaxiality for a different set of compounds given in the inset.

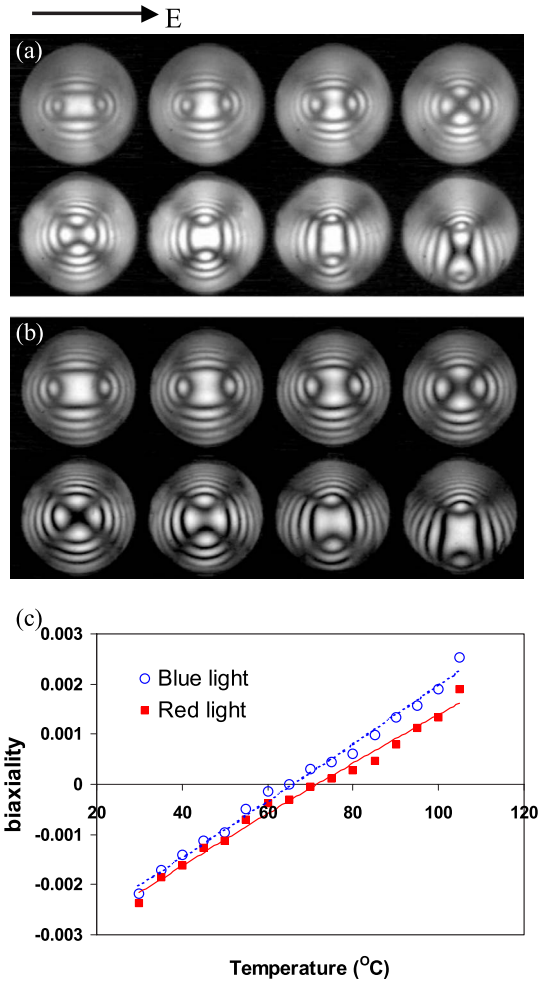

FIG. 7. (Color online) Observed biaxiality dispersions in MC452 for blue and red wavelengths: (a), (b) conoscopic images under blue light (~450 nm) and red light (~600 nm) (MC452, temperature 35,45,…,105 °C (from upper left side)); (c) biaxiality as a function of temperature for blue and red wavelengths. In (a) and (b), the tilt plane is in the vertical direction, whereas the direction normal to the cell is not at the center of the images but is directed at the bottom part of the images.

from a horizontal direction (parallel to the electric field) to a vertical direction (normal to the electric field) with increasing temperature. We also note that this sign reversal of the observed biaxiality in group *B* occurs without the occurrence of sign reversal of the spontaneous polarization or of the helical pitch divergence. Thus, it is quite interesting to elucidate what causes those kinds of behaviors, considering that the Sm-*C* phase is believed to have only positive biaxiality which decreases with increasing temperature.

It is also meaningful to investigate the color dispersion of the biaxiality. Figure 7 shows the conoscopic images of the compound MC452 (belonging to group *B*) at various temperatures under a blue light (average wavelength 450 nm) and a red light (average wavelength 600 nm), respectively. Uniaxiality appears at a different temperature for each wavelength, which indicates that the biaxiality is determined by two or more different physical origins. In other words, if the zero biaxiality or uniaxiality is due to a perfectly random rotation around the molecular long axis and a perfectly isotropic fluctuation of the long axis, the uniaxiality should not exhibit color dispersion. The existence of the color dispersion of biaxiality at the crossover of uniaxiality indicates that there exist at least two or more physical origins, and these compete with each other to produce the zero value of biaxiality.

Three different physical mechanisms have been considered for the emergence of the biaxiality and these may be superimposed.

(i) The molecular long axis thermally fluctuates anisotropically. The stronger azimuthal fluctuations project the largest polarizability along the molecular long axis onto the $Y' \equiv Y$ direction, while the weaker polar fluctuations project it onto the X' axis. Consequently, this mechanism predicts $n_{Y'} > n_{X'}$ [3,5,22].

(ii) The molecular environment is monoclinic and the molecular rotation around its long axis is biased, giving rise to phase biaxiality, i.e., the *quadrupolar ordering* of the short axes which characterizes molecular biaxiality. When the constituent molecules are chiral and the compound is not racemic, such biased rotations also produce spontaneous polarization in the chiral smectic-*C* phase, (Sm-C^*) i.e., the *dipolar ordering* of the short axes characterizing the molecular transverse dipole moments. The chirality reduces the C_{2h} symmetry of Sm-*C* to the C_2 symmetry of Sm-C^*. As a necessary consequence, the transverse molecular dipoles align at least partially; consequently, the spontaneous polarization emerges along the polar direction, which is parallel to the *Y* axis [1,5,7].

(iii) The induced dipoles in the tilted molecules may not polarize symmetrically because of their particular arrangement in Sm-C^*, and hence the local field may not be parallel to the applied electric field. The tensors of dielectric polarizability and permittivity do not need to have the same eigenaxes, which can cause the biaxiality in liquid crystal systems, except for the *Y* axis. In the monoclinic symmetry, the *Y* axis is fixed, while the other two are color dispersive.

The first two mechanisms (i) and (ii) are coupled to each other through the order parameter *D*. One mechanism could affect the other more or less. The main purpose is to examine the sign of the order parameter concerning the mechanism (ii), and the temperature dependencies of the order parameters for mechanisms (i) and (ii).

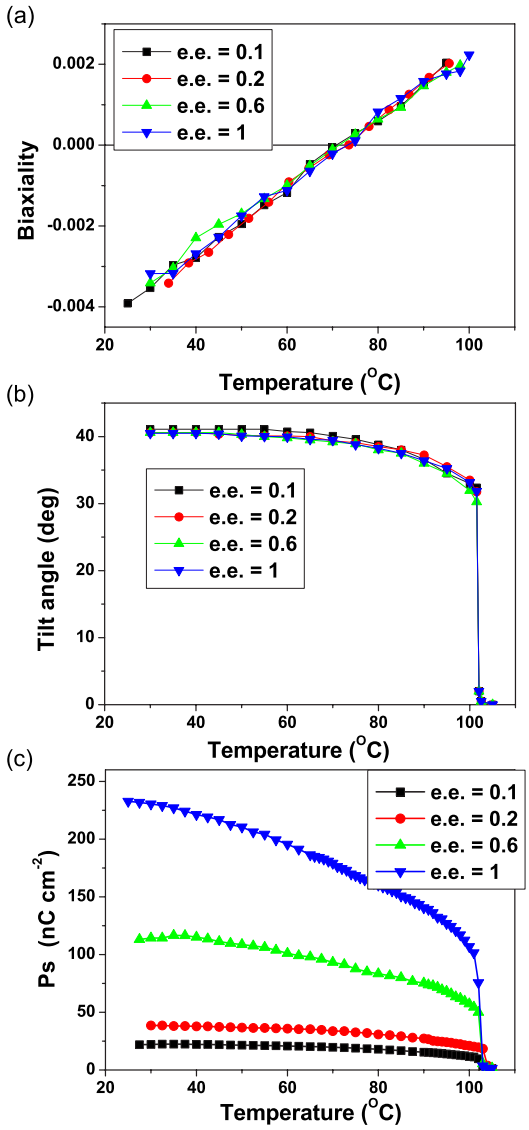

FIG. 8. (Color online) Experimental data for different enantiomeric excess ratios of MC815(*R*) and MC884 (racemate) of the same compound. (a) The observed biaxiality as a function of temperature, (b) the tilt angle as a function of temperature, (c) the spontaneous polarization, P_S as a function of temperature.

C. Observation of biaxiality apparently not dependent on the enantiomeric excess ratios

As already pointed out in Sec. I, it is not so far known whether short-axis ordering was really observed in results about biaxiality, by clearly distinguishing this contribution from those of the long-axis fluctuations, because all the biaxiality observed so far is only positive. The negative biaxiality now observed in Fig. 6 appears to result from the ordering of the short axes. In order to confirm it, let us first experimentally show that, in Sm-C^*, the quadrupolar ordering of the molecular hard cores is sufficiently large as com-

pared with the dipolar ordering of the transverse molecular dipoles. For our experiments, we chose the compound MC815, which is a nominally pure R moiety and shows negative biaxiality, and its racemate MC884. These two compounds are mixed to obtain different enantiomeric excess ratios. Figure 8(a) illustrates the biaxiality vs temperature obtained in several sample compounds with the same chemical structure but different enantiomeric excess (EE) ratios $([R]-[S])/([R]+[S])$, where $[R]$ and $[S]$ represent the amounts by weight of R and S moieties of the compounds contained in the mixture. Surprisingly, in Fig. 8(a), the biaxiality is found to hardly depend on the enantiomeric excess (optical purity) of the sample compounds. The corresponding data on the measured values of the tilt angle and the spontaneous polarization vs temperature are given in Figs. 8(b) and 8(c). The tilt angle is found to be independent of the EE ratio. The accuracy in measuring the biaxiality of unwound Sm-C^* of the nominally optically pure compound was of the order of ±0.0001. When the enantiomeric excess is small, the accuracy in measuring the biaxiality is somewhat reduced by the occurrence of flow, particularly due to the applied electric field. We are in the process of improving the accuracy by using a magnetic field instead of an electric field, so that we can align even the racemate compounds.

The biaxiality measured by conoscopy does not appear to depend on the enantiomeric excess ratio, not only in the high-temperature region, where the biaxiality is positive, but also in the low-temperature region, where it is negative. This means that the chiral intermolecular interactions responsible for producing the spontaneous polarization due to the dipolar ordering are not so strong that they can cause any change in the biaxiality due to the quadrupolar ordering of the molecular hard cores, even in ferroelectric Sm-C^* with rather a large spontaneous polarization. This conclusion apparently contradicts the one obtained by Sigarev *et al.* using ir spectroscopy in Sm-C^* of the compound M5POBC [23]. They analyzed the dependence of the ir absorption of the chiral carbonyl band on the cell rotational angle in terms of its theoretical angular dependence [24], and obtained the distribution function of the biased rotation of the short axis around the long molecular axis in the unwound state. They concluded that the result can be reproduced by assuming dipolar ordering alone. We could not discover the real cause of this discrepancy. When Kim *et al.* unambiguously showed biased rotation of the carbonyl groups in MHPOBC, they noticed the difference in the angular dependencies between the chiral and core carbonyls [25]. They considered that some part of the difference may result from the dipolar ordering of the chiral carbonyl and the quadrupolar ordering of the carbonyl group in the core part of the molecule. Polarized ir absorbance and Raman scattering investigations for a variety of samples of different enantiomeric excess ratios, including those on racemates, would be interesting and valuable in elucidating the ordering of the transverse dipoles responsible for emergence of spontaneous polarization. To detect the dipolar ordering directly, we suggest the use of nonlinear optical techniques, such as coherent Raman scattering and vibrational sum-frequency generation spectroscopy.

IV. DISCUSSION

A. Effective polarizability tensor for modeled D_2 or D_{2h} molecules

Following the above conclusion, we are now allowed to neglect the dipolar ordering and to consider the quadrupolar ordering only. Although the molecules listed in Fig. 1 do not have any symmetry and hence the point symmetry is the C_1 symmetry, we usually model actual molecules as biaxial ones with the point symmetry of D_2 or D_{2h}. We define a right-handed molecular coordinate system with the maximum polarizability z axis, which can also be regarded as the molecular long axis, the minimum polarizability x axis, and the y axis perpendicular to both z and x. Then the molecular polarizability tensor is written as

$$\hat{\boldsymbol{\alpha}}_{\mathrm{mol}} = \begin{pmatrix} \alpha_x & 0 & 0 \\ 0 & \alpha_y & 0 \\ 0 & 0 & \alpha_z \end{pmatrix}. \tag{2}$$

On the other hand, the right-handed Sm-C phase director coordinate system was defined in Sec. I with the Z axis parallel to the director, the Y axis perpendicular to the director tilt plane, and the X axis normal to both Y and Z. It is well known that the ordering of these D_2 or D_{2h} molecules in Sm-C with the phase symmetry of C_{2h} can be specified by four independent order parameters,

$$S = S_{zz}^{Z},$$

$$P = S_{zz}^{Y} - S_{zz}^{X},$$

$$D = S_{yy}^{Z} - S_{xx}^{Z},$$

$$C = (S_{yy}^{Y} - S_{xx}^{Y}) - (S_{yy}^{X} - S_{xx}^{X}). \tag{3}$$

Here, $S_{\alpha\beta}^{i} = \langle (1/2)(3l_{i,\alpha}l_{i,\beta} - \delta_{\alpha\beta}) \rangle$ is one of the three diagonal Saupe ordering matrices, where $l_{i,\alpha}$ is the cosine of the angle between the phase coordinate $i=X$, Y, or Z and the molecular coordinate $\alpha=x$, y, or z [26,27]. In Eq. (3), we defined the P order parameter as $S_{zz}^{Y} - S_{zz}^{X}$, where the Y and X axes are exchanged compared to those in Ref. [27]. This is because we defined the biaxiality as $n_Y - n_X$, which is positive when P is positive. This consideration is required for easily connecting the order parameters to the biaxiality. Note that the P order parameter represents physical mechanism (i), the anisotropic thermal fluctuation of the molecular long axis, and the C order parameter corresponds to physical mechanism (ii), or biased rotation around the molecular long axis.

After averaging the molecular orientation, we can consider that each molecule has, at the center of gravity, the effective polarizability tensor

$$\hat{\boldsymbol{\alpha}} = \begin{pmatrix} \alpha_X & 0 & 0 \\ 0 & \alpha_Y & 0 \\ 0 & 0 & \alpha_Z \end{pmatrix}. \tag{4}$$

The eigenvalues α_i, $i=X$, Y, or Z, are given by

$$\alpha_X = \bar{\alpha} - \frac{1}{3}\left(\Delta\alpha(S+P) + \Delta\alpha_{\perp}\frac{(D+C)}{2} \right)$$

$$\alpha_Y = \bar{\alpha} - \frac{1}{3}\left(\Delta\alpha(S-P) + \Delta\alpha_\perp \frac{(D-C)}{2}\right)$$

$$\alpha_Z = \bar{\alpha} + \frac{2}{3}\left(\Delta\alpha S + \Delta\alpha_\perp \frac{D}{2}\right), \tag{5}$$

where $\bar{\alpha}$ is the average polarizability, and $\Delta\alpha$ and $\Delta\alpha_\perp$ are the anisotropy and the transverse anisotropy of the molecular polarizabilities, respectively [27]. These are given by

$$\bar{\alpha} = (1/3)(\alpha_x + \alpha_y + \alpha_z),$$

$$\Delta\alpha = \alpha_z - (1/2)(\alpha_x + \alpha_y),$$

$$\Delta\alpha_\perp = (\alpha_y - \alpha_x). \tag{6}$$

In fact, Isaert and Billard obtained Eq. (2.3) of Ref. [22] when they examined the anisotropic thermal fluctuations of the molecular long axis. Similarly, we can take the biased rotation around the molecular long axis into account and obtain the effective polarizability tensor in the same form as given in Eq. (4). If we assume perfect nematic order of the long axis, the single order parameter $\langle\cos(2\psi)\rangle$ is needed to calculate α_X, α_Y, and α_Z from α_x, α_y, and α_z. Here, ψ denotes the angle between the X axis and the x axis. In the case of perfect nematic order of the long axis, out of the three biaxial order parameters, only C is finite. It should be noted that the biasing direction is $\psi=0$ or $\pi/2$ in this approximation for the biaxial D_2 or D_{2h} molecule.

B. Local field effect and the resulting positive biaxiality

The anisotropic fluctuation of the molecular long axis and the biased rotation of the molecular short axis around the molecular long axis are the two molecular motions that may primarily cause the emergence of biaxiality in Sm-C. Even if we assume perfect nematic order and free rotation, however, the characteristic layered structure with the tilted director in Sm-C may also produce biaxiality due to the local or effective field effect. We now examine the relation between the effective polarizability tensor with the eigenaxes (X,Y,Z) and the dielectric permittivity tensor with the eigenaxes (X',Y',Z') by considering the local field effect. In general, Z' and X' are not parallel to Z and X, respectively, since these are color dispersive; whereas we can always take $Y' \equiv Y$, since this is fixed. In the approximation of the isotropic local field, which was introduced by Vuks about four decades ago [28,29], we can take $Z' \equiv Z$ and $X' \equiv X$ in addition to $Y' \equiv Y$, and the principal refractive indices can be expressed in terms of polarizabilities as

$$\frac{n_i^2 - 1}{n^2 + 2} = \frac{4\pi N\alpha_i}{3}. \tag{7}$$

Here, α_i and n_i with $i=X$, Y, or Z are the eigenvalues of Eq. (4) and the approximate refractive indices along $i=X$, Y, or Z, respectively, and $n^2=(1/3)(n_X^2+n_Y^2+n_Z^2)$ is the mean square refractive index. N is the number of molecules per cm^3.

The self-consistency of the Vuks equation, Eq. (7), was studied in detail for the uniaxial case, and its validity was established with an accuracy of 0.5% in uniaxial liquid crystalline materials with refractive indices $n_\parallel$ and $n_\perp$ ranging from $\sim$1.46 to $\sim$1.86 [29]. Since the anisotropy Δn is usually much larger than 1%, it is reasonable to assume the isotropic-local-field approximation and to use the Vuks equations in the nematic and Sm-A phases. In the biaxial case of Sm-C under consideration, the transverse anisotropy $\Delta n_\perp$ is of the order of 0.1% and we are not sure whether the isotropic-local-field approximation can quantitatively hold at an accuracy of this level. In order to prove that the negative biaxiality experimentally observed inevitably results from molecular short axis ordering, we now show that the biaxiality due to the local field effect must be positive. Let us use a reasonably simplified model, i.e., the Sm-C phase with perfect nematic order and perfect smectic layer order, consisting of circular-cylindrical hard-rod molecules with length l and diameter a and with the uniaxial effective polarizability tensor $\hat{\boldsymbol{\alpha}}$ at the center of gravity of the molecules, which is written in the (X,Y,Z) coordinate system as

$$\begin{pmatrix} \alpha_\perp & 0 & 0 \\ 0 & \alpha_\perp & 0 \\ 0 & 0 & \alpha_\parallel \end{pmatrix}. \tag{8}$$

Suppose N is the number of molecules per unit volume and $\mathbf{E}'(\mathbf{r},t)$ the local field acting on a particular molecule located at a point $\mathbf{r}$ and at a time t. Then the polarization $\mathbf{P}(\mathbf{r},t)$ is given by

$$\mathbf{P}(\mathbf{r},t) = N\mathbf{p} = N\hat{\boldsymbol{\alpha}}\mathbf{E}'(\mathbf{r},t). \tag{9}$$

Polarization is also written in terms of the mean or observed field $\mathbf{E}(\mathbf{r},t)$ and the dielectric permittivity tensor $\hat{\boldsymbol{\epsilon}}$ as

$$\mathbf{P}(\mathbf{r},\mathbf{t}) = \frac{1}{4\pi}(\hat{\boldsymbol{\epsilon}} - \hat{\mathbf{1}})\mathbf{E}(\mathbf{r},\mathbf{t}). \tag{10}$$

Now we consider a sphere whose center is located at the center of gravity of the particular molecule, and whose radius ρ is sufficiently large compared with the dimensions of the molecule and small enough compared with the wavelength of the incident light. The local field acting on the molecule located at the center of the sphere consists of the sum of two contributions [22,30–32]: one from the outside of the sphere, $\mathbf{E}+(4\pi/3)\mathbf{P}$, and the other from the inside of the sphere, written as

$$\mathbf{E}'(\mathbf{r},t) = \mathbf{E}(\mathbf{r},t) + \frac{4\pi}{3}\mathbf{P}(\mathbf{r},t-\rho/c) + \frac{1}{N}\sum_i \boldsymbol{\nabla}\times\boldsymbol{\nabla} \times \frac{\mathbf{P}(\mathbf{r}_i,t-R_i/c)}{R_i}. \tag{11}$$

Here $R_i=|\mathbf{r}-\mathbf{r}_i|$, and the summation is performed over the molecules inside the sphere. Because of the chosen size of the sphere, we can neglect the retardation effect, replace the summation by integration, and obtain

$$\mathbf{E}'(\mathbf{r},t) = \mathbf{E}(\mathbf{r},t) + \frac{4\pi}{3}(\hat{\mathbf{1}} + \hat{\mathbf{T}})\mathbf{P}(\mathbf{r},t) \tag{12}$$

with

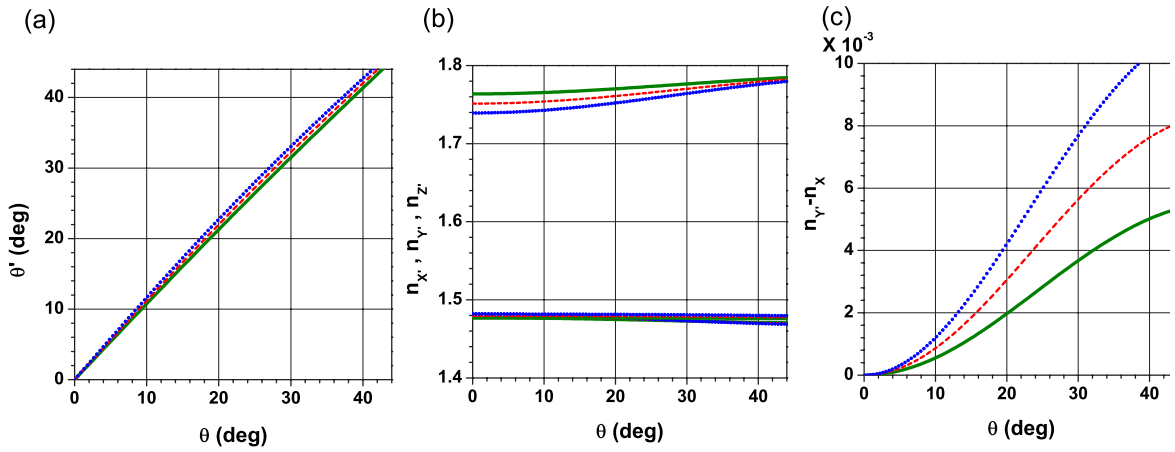

FIG. 9. (Color online) Numerically calculated results for Θ'; $n_{X'}$, $n_{Y'}$, and $n_{Z'}$; and $n_{Y'}-n_{X'}$ as a function of Θ. Parameter values used are $N\alpha_{\parallel}=0.0669$, $N\alpha_{\perp}=0.1011$, $l/a=2$, 3, and 4 [for (green) solid line, (red) dashed, and (blue) dotted, respectively], and 1/50 of the value in Eq. (13).

$$T_{\alpha\beta}=T_{\beta\alpha}=\frac{3}{4\pi}\int\frac{3R_{i\alpha}R_{i\beta}-\delta_{\alpha\beta}R_i^2}{R_i^5}dV', \tag{13}$$

where $R_{i\alpha}=r_\alpha-r_{i\alpha}$ and the integration is to be made by taking into account the excluded volume of the particular molecule located at the center of the sphere. By eliminating $\mathbf{E}'$ and $\mathbf{P}$ with the help of Eqs. (9), (10), and (12), we finally obtain

$$\hat{\boldsymbol{\epsilon}}=\left(\hat{\mathbf{1}}-\frac{4\pi N}{3}\hat{\boldsymbol{\alpha}}(\hat{\mathbf{1}}+\hat{\mathbf{T}})\right)^{-1}\left(\hat{\mathbf{1}}+\frac{4\pi N}{3}\hat{\boldsymbol{\alpha}}(\hat{\mathbf{2}}-\hat{\mathbf{T}})\right). \tag{14}$$

In this way we can calculate $\hat{\boldsymbol{\epsilon}}$ as a function of $N\hat{\boldsymbol{\alpha}}$ [22,32].

Concerning the integration given by Eq. (13) in the isotropic case, it is assumed, as may actually be shown for a number of important special cases, that no resulting field is produced at the central molecule. In the case of Sm-C, on the other hand, the integration plays an essential role for the emergence of biaxiality, and how to determine it is the main issue. Isaert and Billard [22] made the integration using the reasonably simplified model described above [Eq. (8)]. Since uniformly distributed dipoles within a smectic layer of perfect order produce an electric field only in the layer [33,34], as in the case of a plane parallel condenser, we can integrate the field and obtain

$$\hat{\mathbf{T}}=\begin{pmatrix}H & 0 & 0\\ 0 & G & 0\\ 0 & 0 & -G-H\end{pmatrix}. \tag{15}$$

Here G and H are the elliptic functions and are given in Appendix A in the expanded form as functions of l/a and Θ. The integration is performed in the laboratory coordinate system with the axis 3 parallel to the smectic layer normal, the axis 2 perpendicular to the director tilt plane, and the axis 1 normal to both 2 and 3. Accordingly, we inversely transform Eq. (8) written in the director coordinate system (X,Y,Z) into

$$\hat{\mathbf{R}}^{-1}\begin{pmatrix}\alpha_\perp & 0 & 0\\ 0 & \alpha_\perp & 0\\ 0 & 0 & \alpha_\parallel\end{pmatrix}\hat{\mathbf{R}} \tag{16}$$

with the rotation matrix

$$\hat{\mathbf{R}}(\Theta)=\begin{pmatrix}\cos\Theta & 0 & -\sin\Theta\\ 0 & 1 & 0\\ \sin\Theta & 0 & \cos\Theta\end{pmatrix}. \tag{17}$$

Inserting Eqs. (16) and (15) into Eq. (14), we obtain

$$\hat{\boldsymbol{\epsilon}}=\begin{pmatrix}\epsilon_{11} & 0 & \epsilon_{13}\\ 0 & \epsilon_{22} & 0\\ \epsilon_{31} & 0 & \epsilon_{33}\end{pmatrix}, \tag{18}$$

where $\epsilon_{\alpha\beta}$ is given in Appendix B as a function of G, H, $N\alpha_{\parallel}$, $N\alpha_{\perp}$, and Θ.

It should be noted that, in the laboratory frame, the director tilt produces nonzero nondiagonal elements of the dielectric permittivity tensor, which may be diagonalized by a rotation of the coordinate system in the director tilt plane by an angle of Θ'. The angle Θ' is given by

$$\tan 2\Theta'=\frac{\tan 2\Theta}{1-\frac{1}{3}(G+2H)\varkappa}, \tag{19}$$

with

$$\varkappa\equiv\frac{N\alpha_\parallel\alpha_\perp}{(\alpha_\parallel-\alpha_\perp)\cos 2\Theta}, \tag{20}$$

and the relations between the eigenvalues of tensor $\hat{\boldsymbol{\epsilon}}$ and its elements in the laboratory frame are given by

$$n_{X'}^2=\epsilon_{X'}=\frac{1}{2}\left(\epsilon_{33}+\epsilon_{11}-\frac{(\epsilon_{33}-\epsilon_{11})}{\cos 2\Theta'}\right),$$

$$n_{Y'}^2=\epsilon_{Y'}=\epsilon_{22},$$

$$n_{Z'}^2 = \epsilon_{Z'} = \frac{1}{2}\left(\epsilon_{33} + \epsilon_{11} + \frac{(\epsilon_{33} - \epsilon_{11})}{\cos 2\Theta'}\right). \tag{21}$$

Note the relation that exists between the principal refractive indices and the eigenvalues of the dielectric permittivity tensor.

When we numerically obtain the refractive indices n'_X, n'_Y, and n'_Z for suitably assumed parameter values $N\alpha_{\|}=0.0669$, $N\alpha_{\perp}=0.1011$, $\Theta=35°$, and $l/a=2-4$, we notice that the model by Isaert and Billard [22] clearly overestimates the Sm-C anisotropy, and that 1/50 of the value in Eq. (13) reproduces the $\sim 10^{-3}$ level biaxiality actually observed, as shown in Fig. 9. Note that the assumed values of $N\alpha_{\perp}$ and $N\alpha_{\|}$ are obtained from Eq. (7) using the typical values of $n_{\perp}=1.5$ and $n_{\|}=1.7$. Because of the simplified assumptions of the point dipole moment approximation, as well as the perfect nematic orientational and smectic layer order, overestimation of the Sm-C anisotropy is naturally anticipated. Vuks assumed an isotropic local field, which is possible in the isotropic state. The reason that his assumption is valid with quite high accuracy is that real molecules are quite different from point dipoles. The charge is distributed in a complicated way over the entire volume of the molecule, with the dipoles distributed over the molecule. This is closer to an isotropic state. Our assumption, that is, molecules are just point dipoles and the dipole moments are located at the center of the smectic layers in the absence of any fluctuations, gives rise to this overestimation of biaxiality. Even though our calculations cannot yield a quantitative value for the contribution to the biaxiality due to the local field, the calculation process is correct conceptually and yields important qualitative information. Sm-C anisotropy always produces positive biaxiality, $n'_Y > n'_X$. So we are sure that the negative biaxiality experimentally observed unambiguously results from molecular short axis ordering, because both of the remaining causes for the emergence of the biaxiality, i.e., molecular long axis fluctuations and the local field effect, always cause positive biaxiality. Consequently, we keep using the approximation of the isotropic local field for qualitatively analyzing the biaxiality in the following.

C. Quadrupolar ordering of molecular hard cores for C_1 molecules

In the approximation of the isotropic local field, we can write the biaxiality by using Eqs. (4)–(7) as

$$n_Y - n_X = \frac{4\pi N}{3}\frac{n^2+2}{2n_{\perp}}(\alpha_Y - \alpha_X)$$
$$= \frac{4\pi N}{9}\frac{n^2+2}{2n_{\perp}}(2\Delta\alpha P + \Delta\alpha_{\perp} C), \tag{22}$$

where $n_{\perp}=(n_Y+n_X)/2$ is the averaged transverse refractive index. Thus, the biaxiality for biaxial molecules can be described as the sum of mechanisms (i) and (ii), that is, P and C. The order parameter P represents the anisotropic thermal fluctuations of the molecular long axis and is always positive, as already pointed out above; hence, the first term in the last line of Eq. (22) is positive because $\Delta\alpha > 0$ by its definition. Since α_x is the minimum polarizability, $\Delta\alpha_{\perp}$ is also positive, as is clear from Eq. (6). Consequently, to get negative biaxiality, the order parameter C should be negative, which is related to the biased molecular rotation around the long axis. Moreover, considering that the coefficient $2\Delta\alpha$ of the P order parameter is one order of magnitude higher than the coefficient $\Delta\alpha_{\perp}$ of the C order parameter, we can conclude that the absolute value of the C order parameter must be at least ten times larger than that of the P order parameter at low temperatures. This conclusion is consistent with the results obtained by Ossowska-Chrusciel *et al.* [35] in Sm-C^* of MHOBS5 using polarized ir absorbance. Furthermore, they showed that the C order parameter decreases linearly with increasing temperature in Sm-C^* to almost zero near the transition temperature to Sm-A, and that the P order parameter stays almost constant and very small. Thus, we can conclude that the temperature dependence of the biaxiality is determined mainly by a change in the C order parameter, except for the rather steep increase observed in the high-temperature region just below the Sm-A region, which appears to result from a change in the P order parameter. Materials having the order parameter C positive exhibit biaxiality decreasing with increasing temperature, because C is positive and decreases with increasing temperature. On the contrary, materials having the order parameter C negative exhibit biaxiality increasing with increasing temperature, because the absolute value of C deceases with increasing temperature, i.e., the negative order parameter C increases with temperature. The sign reversal of the biaxiality observed in materials having negative C is easily explained. At high temperatures, the positive$P$ contribution is larger than the C contribution, so that the apparent biaxiality is positive. However, at low temperatures, the C contribution is larger than the P contribution, so the biaixiality is negative. At a certain temperature, the two contributions cancel each other out and the biaxiality becomes zero.

For the modeled molecules with D_2 or D_{2h} point symmetry, the biasing of molecular rotation around the long axis in the C_{2h} Sm-C phase symmetry always occurs in such a way that their flat hard cores tend to be either parallel or perpendicular to the director tilt plane. This is why the effective polarizability tensor has the eigenaxes X, Y, and Z, as given in Eq. (4). In the case of perfect nematic order, the biasing direction is $\psi=0$ (x is directed along the X axis) or $\pi/2$ (x is directed along the Y axis). When the X axis is the biasing direction, the biaxiality is positive; whereas it is negative at least at low temperatures when the biasing occurs along the Y axis. Since all of the compounds investigated must have more or less flat hard cores, as the molecular structures listed in Fig. 1 indicate, it is natural to expect that the biasing may occur in the same manner, i.e., parallel only or perpendicular only, for all the compounds. Actually, however, some materials show positive biaxiality due to perpendicular biasing, while some others show negative biaxiablity due to parallel biasing. Some materials show very steep dependence of biaxiality, whereas others (for example, 3.b.5) show a linear increase or decrease with temperature. We intuitively expect that the C order parameter could be close to zero, as well as positive or negative. Zero C apparently means that, in contradiction to the emergence of a large spontaneous polariza-

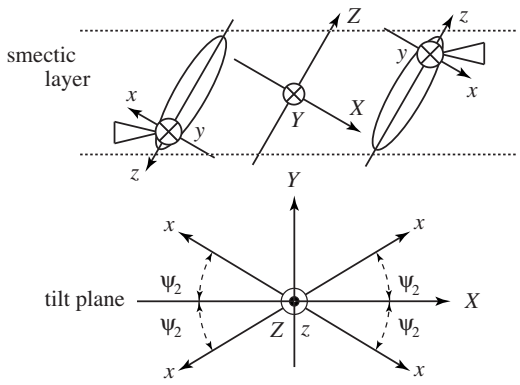

FIG. 10. Schematic illustration of the quadrupolar ordering of molecules with the C_1 point symmetry in the C_2 phase symmetry of the Sm-C^* phase. Upper image: The molecular coordinates x,y,z and the liquid crystal coordinates X,Y,Z are defined as described in text. In the approximation of perfect nematic and smectic orders, molecules are rotating around the $Z \equiv z$ axis. The angle between the X and x axes is ψ, and the triangles schematically represent the transverse dipole moments responsible for spontaneous polarization. Lower image: Biasing directions of molecules with the C_1 point symmetry in the C_2 phase symmetry of Sm-C^* produce quadrupolar ordering of the molecular short axis. See Ref. [25] for the dipolar ordering.

tion, the flat hard core is rotating freely. The discrepancy results from the D_2 or D_{2h} symmetry of the modeled molecules.

All the molecules listed in Fig. 1 have no symmetry and hence the point symmetry is C_1. We can distinguish the head and tail of each molecule, although the number of head-up molecules is equal to that of head-down molecules in Sm-C. For the sake of simplicity, we assume perfect nematic order in the following. The biasing direction of both molecules is generally neither parallel nor perpendicular to the Y axis. Because of the symmetry, the head-up and head-down molecules are biased as illustrated in Fig. 10. The distribution function can be written as

$$f(\psi) = f_{\mathrm{up}}(\psi) + f_{\mathrm{down}}(\psi) = \frac{1}{2(1+a_2)\pi}[1 + a_2 \cos^2(\psi - \psi_2)] + a_2 \cos^2(\psi + \psi_2). \quad (23)$$

The biaxiality is negative for $\psi_2 > \pi/4$, while it is positive for $\pi/4 > \psi_2 > 0$; the changeover occurs continuously at $\psi_2 = 0$, where the system appears uniaxial.

V. CONCLUSION

Using conoscopy and a tilted cell geometry, two types of temperature dependencies of biaxiality have been observed in the perfectly unwound state of the helix in the ferroelectric phase: one decreasing and the other increasing with increasing temperature. In a second class of compounds, the biaxiality at low temperatures is negative, and sign reversal of this was also observed. To find the origin of these behaviors, we have combined the three physical mechanisms that are the conceivable origins for the emergence of biaxiality in a model liquid crystal system composed of rigid calamitic biaxial molecules, with the eigenaxes of the molecular polarizabilities as the long and the short axes [5]. We show that the fluctuations of the long axes and the local field effect can give rise to only one type of biaxiality. By means of a simple theoretical investigation, we find that the average direction of the shortest axis of molecular polarizability, either perpendicular or parallel to the tilt plane, determines the temperature dependence of the biaxiality. If the biasing of the shortest axis is normal to the tilt plane, the biaxiality is negative, and if it is in the tilt plane, it is positive. The short axis ordering is determined by the C order parameter. MHPBC, Felix 18, 3.b.5, C6, and DOBAMBC belong to the positive C order parameter group (positive biaxiality), and MC815, MC452, MC514, MHPOOCBC, Y102, and Tokyo mixture to the negative C order parameter group (negative biaxiality). In actual molecules, a number of conformations of the core part must be possible, and their population may influence the overall biaxiality. Intuitively, however, we can envisage that the central phenyl ring plane of molecules on the average tends to align close to the tilt plane in the latter and out of the tilt plane in the former. The shortest axis normal to the plane of the central phenyl rings is the axis of minimum polarizability. As a result of the competition between the anisotropic fluctuations of the molecular long axis and the biased rotation around the molecular long axis, the unexpected temperature-induced sign reversal of biaxiality observed in the latter group of compounds is explained.

Until now, we do not know what determines whether a liquid crystal material has positive or negative C order parameter. For example, it is quite interesting to note that all molecules having F lateral part, among the materials we used in this experiment, have negative C order parameter. The molecular structure surely affects the orientation of the short axis of the molecule in the smectic phase, but the details still remain to be elucidated in future work. We also conclude that no discrepancy exists in assigning the V-shaped switching materials as Sm-C^* phase rather than the ferrielectric phase assigned initially. In the unwound Sm-C^* phase, the melatopes in conoscopy can appear parallel or perpendicular to the tilt plane.

More recently, Osipov and Pikin [1] theoretically considered the influence of the molecular biaxiality on the ferroelectric properties of Sm-C^* in detail. By using the two order parameters, the molecular long axis and the short axis, they successfully showed that the short molecular axis ordering as well as long axis ordering are both equally important for the phase biaxiality and for a determination of the various ferroelectric properties.

ACKNOWLEDGMENTS

We extend our grateful thanks to Mitsubishi Gas Chemical Company for donating their valuable LCD materials. We thank Ken Ishikawa of Tokyo Institute of Technology for discussions on the optics of the tilted conoscopic experiment. We acknowledge the Science Foundation of Ireland (SFI)

Grant No. 02/IN.1/I.031 for funding the research work in Dublin. J.K.S. thanks Samsung Electronics Co., Ltd. for granting a leave of absence from Seoul. A.V.E. gratefully acknowledges the support of RFBR Grant No. 06-03-08170 and of Russian Ministry of Science Grant No. MK-2034.2006.2. We sincerely thank Professor B. K. Sadashiva synthesizing compound (3.b.5). We acknowledge with thanks the grant SFI 06/RFP/ENE039.

APPENDIX A: CALCULATION OF THE AVERAGE DIPOLE-DIPOLE INTERACTION BETWEEN NONCORRELATED MOLECULES LOCATED WITHIN THE SAME TILTED SMECTIC LAYER

The intersection of a circular-cylindrical molecule and a plane parallel to the smectic layer is an ellipse with semiaxes a and $a/\cos\Theta$, and the coordinates of any point $\mathbf{r}=\{u,v\}$ on this ellipse in the coordinate system parallel to the semiaxes, satisfy the equation

$$u^2 + v^2\cos^2\Theta = a^2. \tag{A1}$$

We need to integrate the dipole-dipole interaction from this elliptic line to the radius ρ of the hypothetical sphere, which can be regarded in practice as infinity, since the integrated result decays in proportion to $\sim 1/r$. Introducing the polar coordinates $\{R,\phi\}$ according to

$$u = R\cos\phi \quad \text{and} \quad v = R\sin\phi, \tag{A2}$$

we obtain from Eq. (A1) the following expression for the distance from the center of the ellipse to the point at the elliptic line $R(\phi)$:

$$[a/R(\phi)] = (\cos^2\phi + \cos^2\Theta\,\sin^2\phi)^{1/2}. \tag{A3}$$

The average dipole-dipole interaction within the layer is then determined by the following integral:

$$\begin{aligned}
&-\int_0^{2\pi} d\phi \int_{R(\phi)}^{\infty} r\,dr\left(\frac{\delta_{\alpha\beta}}{r^3} - \frac{3r_\alpha r_\beta}{r^5}\right) \\
&= -\int_0^{2\pi} d\phi \frac{1}{R(\phi)}(\delta_{\alpha\beta} - 3u_\alpha u_\beta\cos^2\phi - 3v_\alpha v_\beta\sin^2\phi) \\
&= -\frac{1}{a}\int_0^{2\pi} d\phi(1-\sin^2\Theta\,\sin^2\phi)^{1/2} \\
&\quad\times(\delta_{\alpha\beta} - 3u_\alpha u_\beta\cos^2\phi - 3v_\alpha v_\beta\sin^2\phi),
\end{aligned} \tag{A4}$$

where $\mathbf{u}$ and $\mathbf{v}$ are the unit vectors along the semiaxes of the ellipse, which are also parallel to the laboratory frame axes 1 and 2, respectively. Expanding the expression in square brackets in Eq. (A4) in Taylor series with respect to $\sin^2\Theta$, integrating every resulting term with respect to angle ϕ, and substituting the final result into Eq. (13), one obtains G and H for the tensor $\hat{\mathbf{T}}$,

$$G = \frac{3\ell}{4a}\cos\Theta\sum_{k=0}^{\infty}\frac{1}{k+1}\left(\frac{(2k-1)!!}{(2k)!!}\right)^2\sin^{2k}\Theta \tag{A5}$$

and

$$H = -\frac{3\ell}{4a}\cos\Theta\sum_{k=0}^{\infty}\frac{4k+1}{(k+1)(2k-1)}\left(\frac{(2k-1)!!}{(2k)!!}\right)^2\sin^{2k}\Theta. \tag{A6}$$

In Eqs. (A5) and (A6), it is assumed for convenience that the double factorial of any negative or zero integer number is equal to 1. By contrast with the previous paper [22], we have not obtained any terms independent of the molecular dimension, probably because we disregarded the positional correlation of molecules in the neighboring layers. Correct consideration of positional correlation is difficult. At the same time, in the case of the calamitic mesogenic molecules, this positional correlation produces only small additional terms in Eqs. (A5) and (A6).

APPENDIX B: COMPONENTS OF THE DIELECTRIC PERMITTIVITY TENSOR IN THE LABORATORY FRAME

The expressions for ϵ_{ij} in Eq. (18) are as follows:

$$\begin{aligned}
\epsilon_{11} = \frac{1}{\Delta}\Bigg(1 + \frac{4\pi}{3}&[(2-H)(N\alpha_\perp\cos^2\Theta + N\alpha_\parallel\sin^2\Theta) \\
&- (1-G-H)(N\alpha_\perp\sin^2\Theta + N\alpha_\parallel\cos^2\Theta)] \\
&- \frac{16\pi^2}{9}(2-H)(1-G-H)N\alpha_\parallel N\alpha_\perp\Bigg),
\end{aligned} \tag{B1}$$

$$\epsilon_{22} = \frac{1 + (4\pi/3)N\alpha_\perp(2-G)}{1-(4\pi/3)N\alpha_\perp(1+G)}, \tag{B2}$$

$$\begin{aligned}
\epsilon_{33} = \frac{1}{\Delta}\Bigg(1 + \frac{4\pi}{3}&[(2+G+H)(N\alpha_\perp\sin^2\Theta + N\alpha_\parallel\cos^2\Theta) \\
&- (1+H)(N\alpha_\perp\cos^2\Theta + N\alpha_\parallel\sin^2\Theta)] \\
&- \frac{16\pi^2}{9}(1+H)(2+G+H)N\alpha_\parallel N\alpha_\perp\Bigg),
\end{aligned} \tag{B3}$$

$$\epsilon_{13} = \epsilon_{31} = \frac{2\pi}{\Delta}(N\alpha_\perp - N\alpha_\parallel)\sin 2\Theta, \tag{B4}$$

where

$$\begin{aligned}
\Delta = 1 - \frac{4\pi}{3}&[(1+H)(N\alpha_\perp\cos^2\Theta + N\alpha_\parallel\sin^2\Theta) + (1-G-H) \\
&\times(N\alpha_\perp\sin^2\Theta + N\alpha_\parallel\cos^2\Theta)] \\
&+ \frac{16\pi^2}{9}(1+H)(1-G-H)N\alpha_\parallel N\alpha_\perp.
\end{aligned} \tag{B5}$$

[1] M. A. Osipov and S. A. Pikin, J. Phys. II **5**, 1223 (1995).
[2] A. Saupe, Mol. Cryst. Liq. Cryst. **7**, 59 (1969).
[3] T. R. Taylor, J. L. Fergason, and S. L. Arora, Phys. Rev. Lett. **24**, 359 (1970).
[4] T. R. Taylor, S. L. Arora, and J. L. Fergason, Phys. Rev. Lett. **25**, 722 (1970).
[5] Y. Galerne, J. Phys. (Paris) **39**, 1311 (1978).
[6] N. A. Clark and S. T. Lagerwall, Appl. Phys. Lett. **36**, 899 (1980).
[7] R. B. Meyer, L. Liebert, L. Strzelecki, and P. Keller, J. Phys. (Paris), Lett. **36**, L69 (1975).
[8] E. Gorecka, A. D. L. Chandani, Y. Ouchi, H. Takezoe, and A. Fukuda, Jpn. J. Appl. Phys., Part 1 **29**, 131 (1990).
[9] A. Fukuda, Y. Takanishi, T. Isozaki, K. Ishikawa, and H. Takezoe, J. Mater. Chem. **4**, 997 (1994).
[10] P. M. Johnson, D. A. Olson, S. Pankratz, T. Nguyen, J. Goodby, M. Hird, and C. C. Huang, Phys. Rev. Lett. **84**, 4870 (2000).
[11] A. V. Emelyanenko, A. Fukuda, and J. K. Vij, Phys. Rev. E **74**, 011705 (2006).
[12] T. Matsumoto, A. Fukuda, M. Johno, Y. Motoyama, T. Yui, S.-S. Seomun, and M. Yamashita, J. Mater. Chem. **9**, 2051 (1999).
[13] M. Takeuchi, K. Chao, T. Ando, T. Matsumoto, A. Fukuda, and M. Yamashita, Ferroelectrics **246**, 1 (2000).
[14] Y. Yoshioka, M. Johno, T. Yui, and T. Matsumoto, European Patent Application No. EP1039329 (2000).
[15] D. W. Berreman, Mol. Cryst. Liq. Cryst. **22**, 175 (1973).
[16] K. Hori, Mol. Cryst. Liq. Cryst. **100**, 75 (1983).
[17] Y. Ouchi, T. Shingu, H. Takezoe, A. Fukuda, E. Kuze, M. Koga, and N. Goto, Jpn. J. Appl. Phys., Part 2 **23**, L660 (1984).
[18] A. Fukuda, in *Proceedings of the Fifth International Display Research Conference, Hamamatsu, Japan 1995 (Asia Display 95)* (Institute of Television Engineering of Japan, the Society for Information Display, Tokyo, 1995).
[19] S. Inui, N. Iimura, T. Suzuki, H. Iwase, K. Miyachi, Y. Takanishi, and A. Fukuda, J. Mater. Chem. **6**, 671 (1996).
[20] J. K. Song, A. D. L. Chandani, O. E. Panarina, A. Fukuda, J. K. Vij, V. Goertz, and J. W. Goodby, Ferroelectrics **344**, 41 (2006).
[21] V. P. Panov, B. K. McCoy, Z. Q. Liu, J. K. Vij, J. W. Goodby, and C. C. Huang, Phys. Rev. E **74**, 011701 (2006).
[22] N. Isaert and J. Billard, Mol. Cryst. Liq. Cryst. **38**, 1 (1977).
[23] A. A. Sigarev, J. K. Vij, A. Fukuda, B. Jin, and Y. Takanishi, Ferroelectrics **311**, 97 (2004).
[24] W. G. Jang, C. S. Park, J. E. Maclennan, K. H. Kim, and N. A. Clark, Ferroelectrics **180**, 213 (1996).
[25] K. H. Kim, K. Ishikawa, H. Takezoe, and A. Fukuda, Phys. Rev. E **51**, 2166 (1995).
[26] C. Zannoni, *The Molecular Physics of Liquid Crystals* (Academic Press, London, 1979), Chap. 3.
[27] D. Dunmur and K. Toriyama, *Handbook of Liquid Crystals*, Vol. 1 (Wiley-VCH, Weinheim, 1998), Chap. 7, p. 199.
[28] M. F. Vuks, Opt. Spektrosk. **20**, 644 (1966).
[29] J. Li and S. T. Wu, J. Appl. Phys. **96**, 6253 (2004).
[30] H. E. J. Neugebauer, Can. J. Phys. **32**, 1 (1954).
[31] H. S. Subramhanyam and D. Krishnamurti, Mol. Cryst. Liq. Cryst. **22**, 239 (1973).
[32] M. Born and E. Wolf, *Principles of Optics* (Cambridge University Press, Cambridge, U.K., 1999), Chap. 2.
[33] M. A. Osipov and A. Fukuda, Phys. Rev. E **62**, 3724 (2000).
[34] J. Prost and R. Bruinsma, Ferroelectrics **148**, 25 (1993).
[35] M. D. Ossowska-Chrusciel, R. Korlacki, A. Kocot, R. Wrzalik, J. Chrusciel, and S. Zalewski, Phys. Rev. E **70**, 041705 (2004).
[36] J. K. Song, J. K. Vij, and I. Kobayashi, Phys. Rev. E **75**, 051705 (2007).